

## **Quantification of green areas: a methodology for monitoring and environmental management**

### **Ramon Octaviano de Castro Matoso**

Environmental and Sanitary Engineer, Master in Geography program, PPGeo, NAGEA, UFJF, Brazil  
ramon.matoso@engenharia.ufjf.br

### **Lucas do Vale Souza**

Geographer, Master in Built Environment program, PROAC, NAGEA, UFJF, Brazil  
lucas.vale@engenharia.ufjf.br

### **César Henrique Barra Rocha**

Professor, Transportation and Geotechnics Department, NAGEA, PPGeo, PROAC, UFJF, Brazil  
barra.rocha@engenharia.ufjf.br

## **ABSTRACT**

The monitoring of green areas has been researched and analyzed by several surveys, however it is not trivial to find data with reliable accuracy and precision. There are well-defined and widely used methodologies for the classification of large area images, but in the case of small areas some authors recommend the analog analysis of aerial photos for classification. However, the acquisition of high definition aerial images is not inexpensive. In addition to being a fully manual and labor intensive classification. The present work proposes a methodology for the collection of a quantitative historical database using remote sensing techniques and Digital images, using the NDVI as a comparison criterion. In this work, free images of the Landsat-5, Landsat-8 and Sentinel-2 satellites were used to verify if it is possible to extract reliable information from areas considered small to use the classification supervised by the maximum likelihood method using the ENVI 5.1 software.

**KEYWORDS:** Remote Sensing, Green Areas, Digital Classification and Soil Coverage.

## **1 INTRODUCTION**

The UN (United Nations) issued the first World Commission on Environment and Development report, titled "Our Common Future" (WCED, 1987), setting guidelines for sustainable development. Duran et al. (2015) claim that, in an analysis of the elements of sustainable development, its economic potential happens through gradual change, while socioeconomic development changes very rapidly, thus creating imbalance. Global action in land use planning therefore requires improved management, as it is an efficient tool in resource usage and demand and it ensures well-organized land use, according to changes in the environment or to the observed socioeconomic circumstances (Nguyen et al., 2015).

The situation in Brazil is concerning. Results of the latest MapBiomass (2019) report show that, in the last few years, increase in deforestation was highest, mainly in the Amazon (rainforest) and Cerrado (savannah) biomes, which account for 96.7% of all deforestation in Brazilian territory. Irregularities were found in 99% of all deforestation detected in 2019, ranging from activity in protected or legally restricted areas to unauthorized suppression of vegetation. Therefore, the importance of protecting remaining native vegetation in Brazil cannot be overstated.

There are several strategies that may help in land use mapping for planning and protection of green space, namely the Normalized Difference Vegetation Index (NDVI). According to Robinson et al. (2017), it is a widely implemented land use mapping tool in remote sensing.

There are several papers in which satellite image-based land-use classification tool use is aided by NDVI, such as Weckmüller et al. (2018), Cabral et al. (2019), Ruiz Durán et al. (2017), and Robinson et al. (2017), with satisfactory results in class differentiation and over 90% accuracy.

## **2 OBJECTIVES**

The aim of this paper is to propose a precise methodology for land use mapping in a drainage basin, using satellite imagery from various agencies combined with remote sensing applications, to ultimately demonstrate that the use of GIS applications may yield relevant results in urban planning and in the conservation of remaining green space.

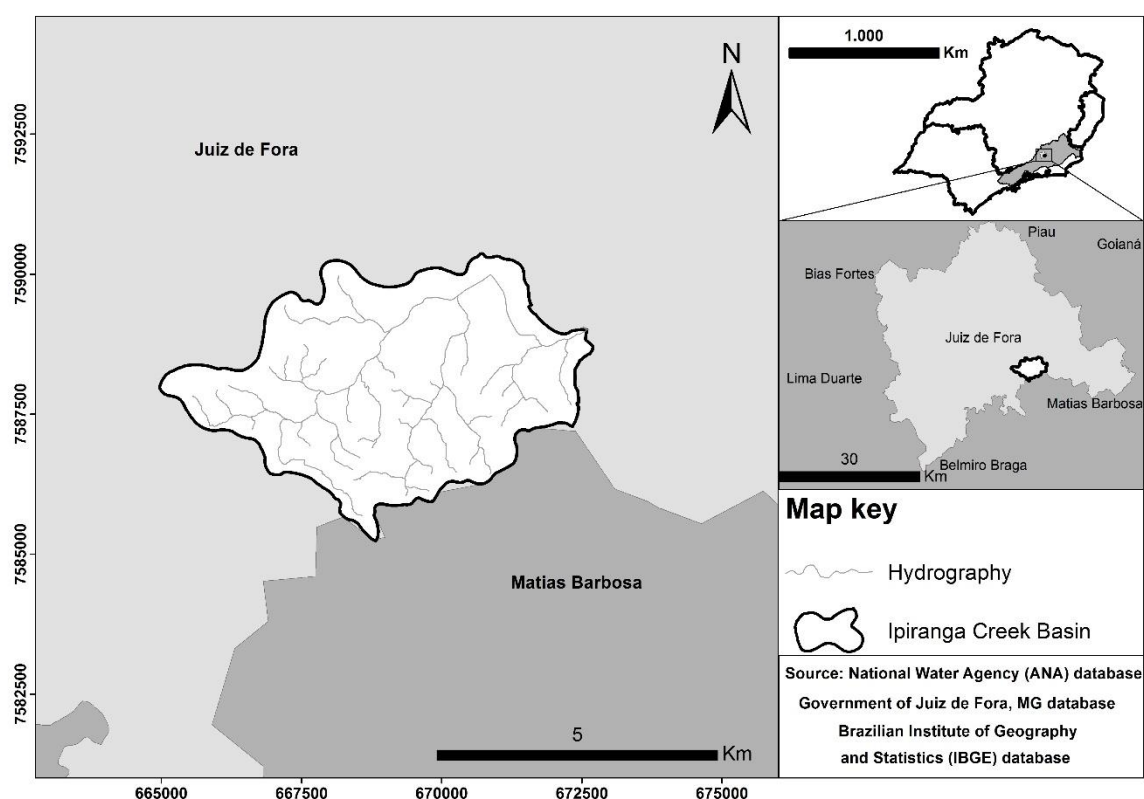
### 3 METHODOLOGY

The methodological procedures of this study consist of the examination of free satellite imagery (Landsat-5, Landsat-8, and Sentinel-2) and the application of mapping algorithms using the maximum likelihood estimation method and the kappa index, which classifies land use mapping as very poor, poor, average, good, very good or excellent. The resulting data were compared to information in scientific papers, so that the vegetation analysis could be categorized by a uniform indicator capable of showing a reasonable sample of the studied location. In short, this paper's methodology is divided in 5 stages: (1) obtaining satellite imagery; (2) describing the bands and band combinations, and creating NDVI; (3) creating the land use map with and without the NDVI band; (4) applying the kappa index to assess the accuracy of the land use and settlement maps; and (5) comparing the results with information provided in the selected papers.

#### 3.1 Study area

The Ipiranga Creek basin area (Figure 1) is located in the city of Juiz de Fora, state of Minas Gerais, Brazil, with a total area of approximately 21.3 km<sup>2</sup>. Marques Neto et al. (2017) describe it as a region with “densely populated plains and terraces and increasingly inhabited hillsides, known for its rather convex ‘sea of hills’ morphology, where both flat and hilly areas are inhabited.” Its land use is highly diversified, with densely built-up areas, pasture, patches of forest and farmland all in one same area (Barra Rocha et al., 2019; De Oliveira et al., 2018).

Figure 1: Map of the Ipiranga Creek drainage basin.



Source: The authors.

### 3.2 Acquisition of satellite imagery and band combinations

All data retrieved in this study derive from free imagery generated by American Landsat and European Sentinel satellites. Sothe et al. (2017) show how such data have improved over the years, with newer series offering better resolution and more information. Currently, Landsat-5, Landsat-8 and, more recently, Sentinel-2 are the most used series. Landsat-5 and Landsat-8 images are made of different bands — the former comes in 7 bands, while the latter comes in 11 bands, as shown in Chart 1.

**Chart 1: Landsat-5 and Landsat-8 spectral bands and spatial resolution.**

LANDSAT-5			LANDSAT-8		
Band	Central Wavelength (µm)	Spatial Resolution (m)	Band	Central Wavelength (µm)	Spatial Resolution (m)
1 (blue)	0.485	30	1 (aerosol)	0.440	30
2 (green)	0.570	30	2 (blue)	0.480	30
3 (red)	0.660	30	3 (green)	0.550	30
4 (NIR)	0.830	30	4 (red)	0.655	30
5 (MIR)	1.655	30	5 (OIR)	0.865	30
6 (FIR)	2.215	30	6 (MIR)	1.610	30
7	11.450	120	7 (FIR)	2.200	30
			8	0.590	15
			9	1.370	30
			10	10.895	100
			11	12.005	100

Source: USGS (2020).

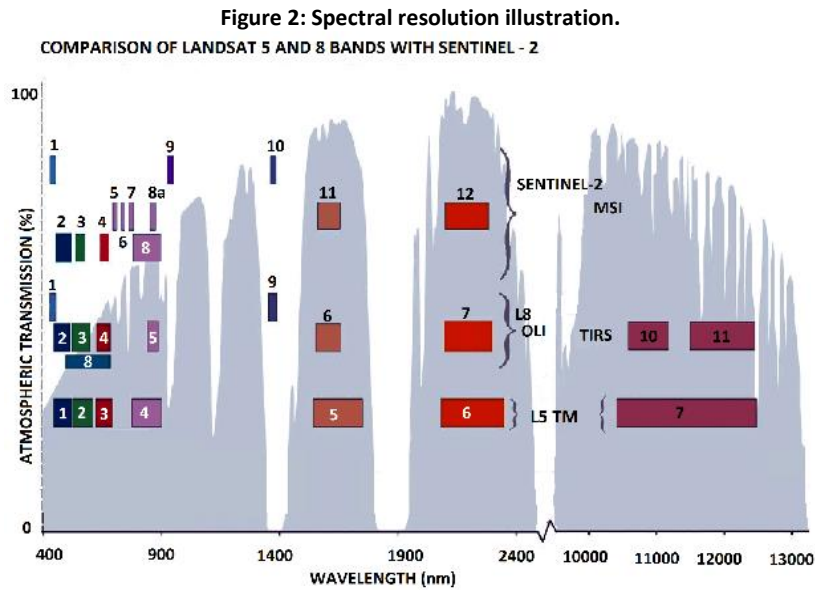
Sentinel-2 images come in 12 bands. Unlike Landsat series, spatial resolution is better in Sentinel-2, providing more accurate imagery. The bands are shown in Chart 2:

**Chart 2: Sentinel-2 spectral bands and spatial resolution.**

Band	Central Wavelength (µm)	Spatial Resolution (m)
1 (aerosol)	0.443	60
2 (blue)	0.490	10
3 (green)	0.560	10
4 (red)	0.665	10
5	0.705	20
6	0.740	20
7	0.783	20
8 (NIR)	0.842	10
8 A	0.865	20
9 (water vapor)	0.945	60
10	1.375	60
11	1.610	20
12	2.190	20

Source: USGS (2020).

Figure 2 indicates each band’s spectral resolution in each satellite model. Bezerra et al. (2018) and Moreira et al. (2020) claim that the spectral values are relatively similar in red bands, while there are more differences among infrared bands, mainly in Landsat-8 and Sentinel-2 models. Therefore, when NDVI is enabled for land-use mapping, this issue yields varying mapping results according to the satellite used in each case.



Source: USGS (2020).

All bands with 30-meter spatial resolution dated 1999-08-12 and 2011-08-13 from Landsat-5 and 2016-07-25 from Landsat-8, as well as 10-meter spatial resolution images dated 2016-07-13 from Sentinel-2, were downloaded. All Landsat series images were obtained from the National Space Research Institute (INPE) image catalog, while Sentinel-2 images were obtained from the United States Geological Survey (USGS) image catalog.

### 3.3 NDVI application

To ensure higher accuracy in classification and quantification of land use classes, the bands were combined using the Normalized Difference Vegetation Index (NDVI), according to the definition given by Rouse et al. (1973).

NDVI is calculated as the ratio between the difference and the sum of near-infrared ( $\rho_{nri}$ ) and red ( $\rho_{red}$ ) reflectance values. The authors of this paper chose to use NDVI due to the fact that vegetation cover absorbance is highest in the red band. Equation 1 represents the calculation (BEZERRA et al., 2018):

$$NDVI = \frac{\rho_{nri} - \rho_{red}}{\rho_{nri} + \rho_{red}} \quad (1)$$

ENVI 5.1 was the choice of software for NDVI application, as defined by Rouse et al. (1973), using near-infrared and red bands to generate NDVI imagery.

After generating NDVI imagery for the aforementioned dates — mostly within the dry season — in all satellites, all the bands were combined, along with NDVI, using the same spatial resolutions as in the images from said dates. ARCGIS 10.2.1 was the software used for band combination. Two images were generated for each date — one with bands only and another with bands and NDVI, for a total of 8 images: 4 from Landsat-5, 2 from Landsat-8, and 2 from Sentinel-2. Chart 3 provides further information on this process.

**Chart 3: Landsat-5, Landsat-8 and Sentinel-2 band combinations.**

Combined bands										
Landsat-5					Landsat-8			Sentinel-2		
Band	Aug. 1999		Aug. 2011		Band	Jul. 2016	Jul. 2016	Band	Jul. 2016	Jul. 2016
	Without NDVI	With NDVI	Without NDVI	With NDVI		Without NDVI	With NDVI		Without NDVI	With NDVI
1	X	X	X	X	1	X	X	1	N/A	N/A
2	X	X	X	X	2	X	X	2	X	X
3	X	X	X	X	3	X	X	3	X	X
4	X	X	X	X	4	X	X	4	X	X
5	X	X	X	X	5	X	X	5	N/A	N/A
6	X	X	X	X	6	X	X	6	N/A	N/A
7	N/A	N/A	N/A	N/A	7	X	X	7	N/A	N/A
NDVI	N/A	X	N/A	X	8	N/A	N/A	8	X	X
					9	X	X	8 A	N/A	N/A
					10	N/A	N/A	9	N/A	N/A
					11	N/A	N/A	10	N/A	N/A
					NDVI	N/A	X	11	N/A	N/A
								12	N/A	N/A
								NDVI	N/A	X

Source: Adapted from USGS (2020).

### 3.4 Land use and settlement

To classify land use and settlement in satellite imagery, ENVI 5.1 software was used with supervised maximum likelihood classification. This method was chosen for its widespread use and for the fact that, when combined with other techniques, it can lead to an improvement of almost 83% in land use classification (SILVEIRA et al., 2020).

### 3.5 Kappa index

After classifying land use and settlement, the level of uncertainty in the maps was checked — accounting for errors in satellite imagery classification procedures — using accuracy indexes to ensure proper use of obtained information. According to Landis and Koch (1977), the kappa coefficient is defined as a measure of association that is used to describe and test the level of agreement (reliability and precision) in land use and settlement classification. Chart 4 identifies agreement level classes for the kappa index.

**Chart 4: Kappa index.**

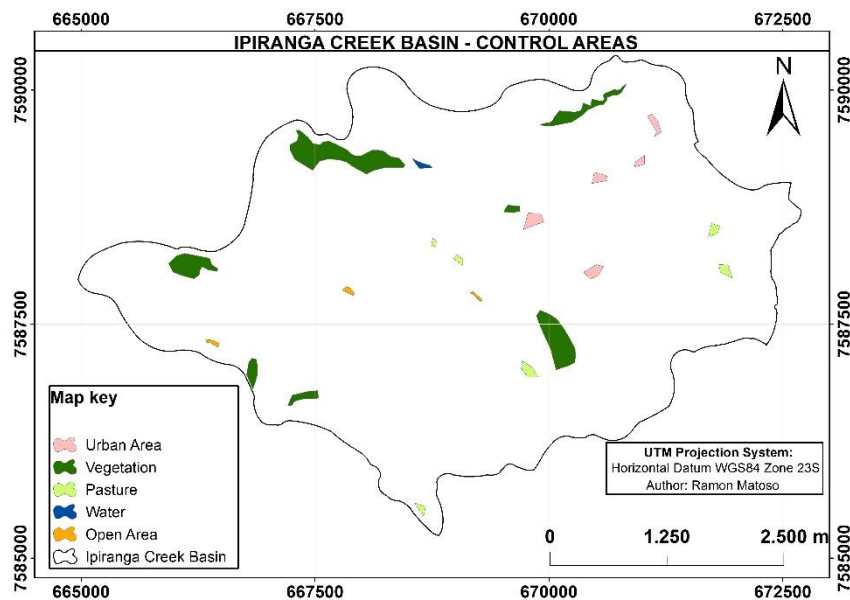
Kappa value	Agreement
<b>0</b>	Very poor
<b>0–0.20</b>	Poor
<b>0.21–0.40</b>	Average
<b>0.41–0.60</b>	Good
<b>0.61–0.80</b>	Very good
<b>0.81–1.00</b>	Excellent

Source: Landis and Koch (1977).

In order to assess the accuracy of land use in Sentinel-2, control areas were defined (as shown in Figure 3). These areas were extracted and validated by Google Earth Pro software. After obtaining said reference areas, the KML file was converted to shapefile. The shapes were then converted to ROI format so they could be read by the comparison tool in ENVI 5.1. The error matrices and the kappa index were generated from the resulting data, and then both classifications were compared to check the level of agreement between the images.

No control points were used to generate the error matrices in 1999, 2011 and 2016 Landsat series images. To assess and discuss the comparative assertiveness between maps, the kappa index and the accuracy were generated using the resulting conflict between classified images from the same dates.

**Figure 3: Map of control areas used in Sentinel-2 to generate kappa index.**



Source: The authors.

## 4 RESULTS AND DISCUSSION

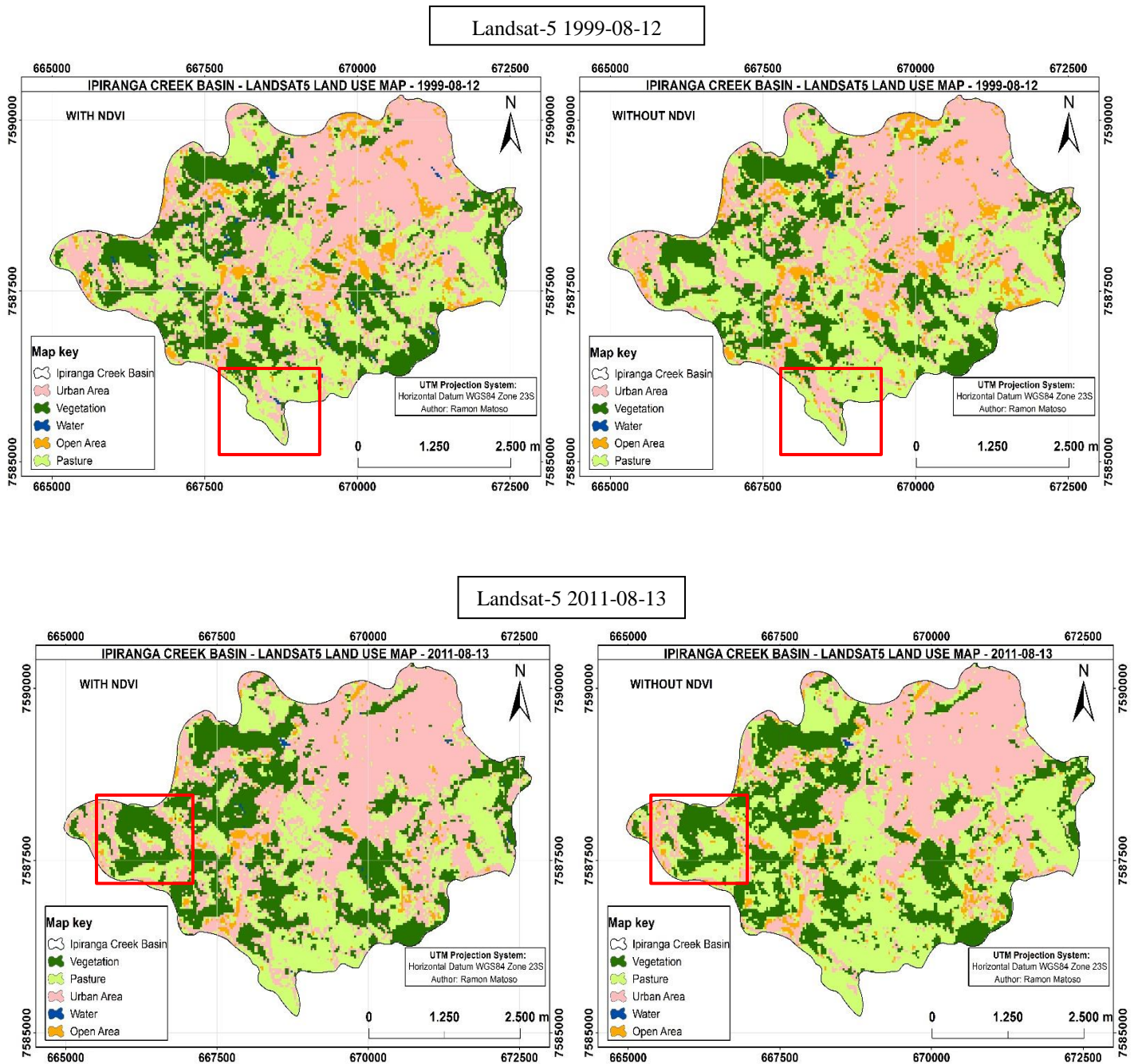
### 4.1 Land use and settlement classification

The generated land use and settlement maps show a difference between images classified with NDVI and those classified without it. In Figure 4, with Landsat-5 data, areas in which NDVI was applied do a better job of distinguishing urban space class from pasture and

forest classes. The points marked with a rectangle represent this visual difference. Image quality, however, is slightly worse than in the other two satellite series.

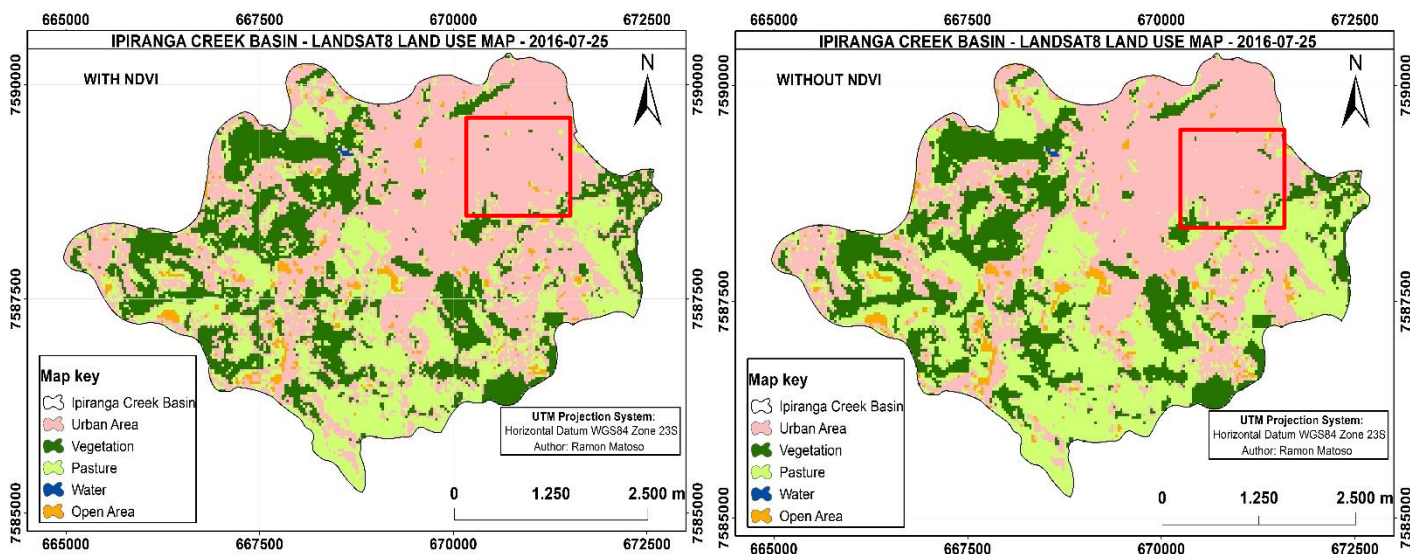
The visual difference is even greater in Figures 5 and 6. Forest, pasture and urban space classes are more homogenous in Landsat-8 images. In contrast, Sentinel-2A images deliver higher precision and make it possible to see smaller areas not seen in other cases due to the accuracy of these images.

Figure 4: Land use map, Landsat-5.



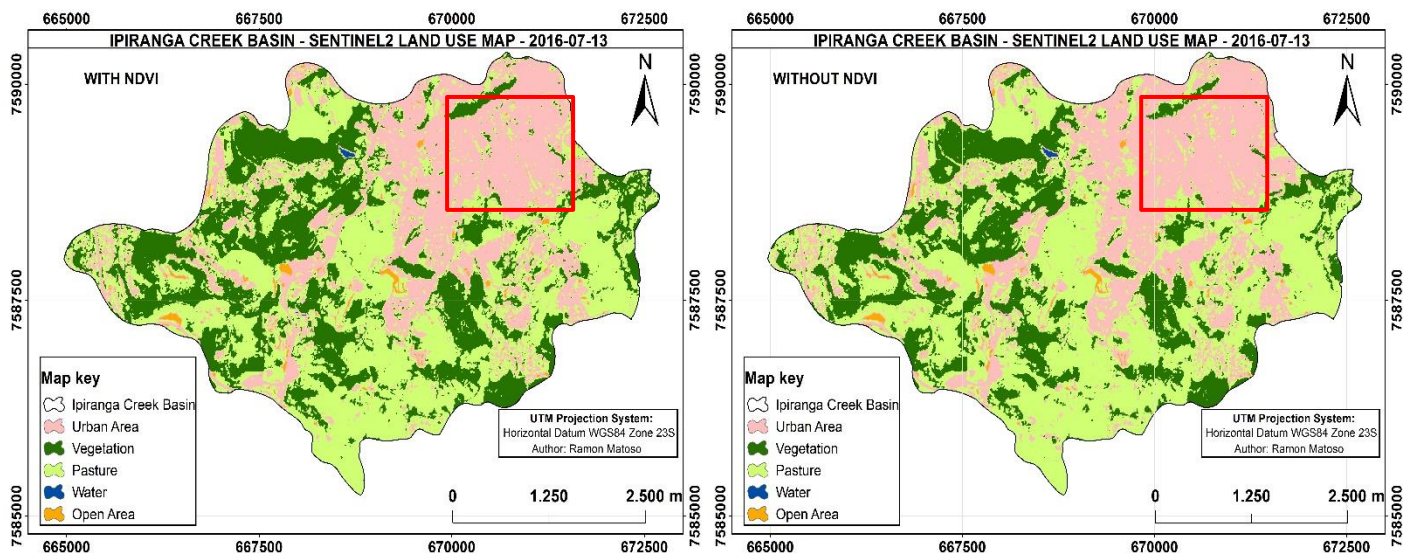
Source: The authors.

Figure 5: Land use map, Landsat-8, 2016-07-25.



Source: The authors.

Figure 6: Land use map, Sentinel-2, 2016-07-13.



Source: The authors.

#### 4.2 Land use and settlement agreement matrices

Sentinel-2 image classification provided the best representation. This was expected, given the superior spatial resolution provided by the channels chosen for classifying the image. The classification of the image that included NDVI in its band combination yielded even better results than the classification of the non-NDVI image. The agreement matrices for Sentinel-2

images classified with and without NDVI can be found in the following charts. Chart 8 shows the level of agreement in both classifications, with control areas extracted from Google Earth Pro.

**Chart 8: Agreement matrix (in pixels) for Sentinel-2A classified image from 2016-07-13.**

Classified Image	Reference data (Google Earth Pro) with NDVI						
	Urban Space	Vegetation	Pasture	Water	Open Area	Total Hits	Total
Urban Space	1369	20	43	7	2	1369	1441
Vegetation	0	8023	2	0	0	8023	8025
Pasture	17	117	2283	0	0	2283	2417
Water	0	0	0	78	0	78	78
Open Area	4	0	3	0	196	196	203
Total	1390	8160	2331	85	198	11949	12164
Classified Image	Reference data (Google Earth Pro) without NDVI						
	Urban Space	Vegetation	Pasture	Water	Open Area	Total Hits	Total
Urban Space	1369	19	42	5	2	1369	1441
Vegetation	0	7319	0	0	0	7319	7319
Pasture	17	822	2286	0	0	2286	3125
Water	0	0	0	80	0	80	80
Open Area	4	0	3	0	196	196	203
Total	1390	8160	2331	85	198	11250	12168

Source: The authors.

The aforementioned chart was built with ENVI 5.1, based on the control areas shown in Figure 3. Classification enhanced by inclusion of NDVI in band combination produced 0.965 and 98.23% for kappa and accuracy, respectively. Classification made from NDVI-disabled band combination produced values of 0.8591 and 92.486% for kappa and accuracy, respectively. According to Landis and Koch (1977), the coherence is excellent in both cases. Chart 9 shows the coherence of both classifications, in direct comparison, for which the values of kappa and accuracy were 0.8613 and 90.9436%. One may notice that the level of assertiveness is higher in the NDVI-enhanced classified image than in its NDVI-disabled counterpart, in which there was vegetation cover/urban space confusion in 0.11% of its pixels (325 pixels in total), as well as vegetation cover/pasture confusion in 13% of its pixels (72,510 pixels in total). Of course, this results in omission of data that are important to the intended quantification. It is notorious that NDVI-enabled classification was indeed highly representative for quantitative purposes, as each pixel in this image accounts for an area of approximately 100 m<sup>2</sup>.

**Chart 9: Agreement matrix (in percentages) for Sentinel-2A classified images from 2016-07-13.**

Classified without NDVI	Classified with NDVI				
	Urban Space	Vegetation	Pasture	Water	Open Area
Urban Space	92.04%	0.94%	0.55%	0.19%	5.02%
Vegetation	0.11%	96.63%	13.00%	0.00%	0.00%
Pasture	7.45%	2.43%	86.45%	0.00%	0.00%
Water	0.03%	0.00%	0.00%	99.81%	0.00%
Open Area	0.37%	0.00%	0.00%	0.00%	94.98%
Total (Pixels)	299278	375662	557647	2053	6379

Source: The authors.

Regarding Landsat imagery data, the classifications were not as refined as those made with Sentinel-2. The Landsat series has a combined band spatial resolution of 30 meters. In other words, a single pixel in these images accounts for an area of 900 m<sup>2</sup>, thus certainly omitting data that are important to said classification. Nonetheless, it is possible to assess how vegetation in the basin has changed by using either a longer timespan or a large-scale drainage basin.

Chart 10 illustrates the conflict in classified Landsat-5 and Landsat-8 images, whose levels of assertiveness may be compared to those in previous classifications. It also shows Landsat-8 coherence values in 2016-07-25. Such conflict yields 0.7263 and 81.4541% for kappa and accuracy, respectively. The chart also indicates the occurrence of many classification errors, of which the greatest ones are in the open areas and pasture classes. There were also errors in vegetation cover classification — in both Landsat-8 instances, there was considerably more conflict than in Sentinel-2. This was expected, as there is greater uncertainty in the former case due to omission of relevant data caused by band spatial resolution. The data in this classification may be compared and validated using the kappa index as a coherence factor.

Chart 10 also shows that the coherence values between the two classified Landsat-5 images in 1999-08-12 were 0.7262 and 80.9645% for kappa and accuracy. This classification is of the same order of assertiveness as the other ones. Hence, in all images, kappa index use is completely reasonable to validate quantitative data extracted from classified imagery.

Chart 11 gives coherence values between the two classified Landsat-5 images from 2011-08-13. In this case, the conflict yielded 0.7475 and 82.5113% for kappa and accuracy. Just like in the last case, classifications on 2011-08-13 yielded the same order of assertiveness, with the greatest errors in pasture and open areas.

**Chart 10: Agreement matrix (in percentages) for LANDSAT-8 and LANDSAT-5 classified images.**

LANDSAT-8 – 2016-07-25					
Classified without NDVI	Classified with NDVI				
	Urban Space	Vegetation	Pasture	Water	Open Area
Urban Space	89.23%	2.94%	26.95%	0.00%	40.39%
Vegetation	1.16%	93.2%	9.07%	0.00%	0.00%
Pasture	7.96%	3.78%	63.88%	0.00%	9.09%
Water	0.08%	0.00%	0.00%	98.83%	0.33%
Open Area	1.09%	0.08%	0.11%	1.17%	50.19%
Total (Pixels)	47108	44541	46612	256	2441
LANDSAT-5 1999-08-12					
Classified without NDVI	Classified with NDVI				
	Urban Space	Vegetation	Pasture	Water	Open Area
Urban Space	82.48%	1.23%	21.61%	6.57%	30.52%
Vegetation	2.81%	94.55%	5.51%	0.00%	3.74%
Pasture	12.52%	0.71%	72.72%	0.00%	11.35%
Water	0.65%	3.51%	0.00%	93.43%	0.20%
Open Area	1.54%	0.00%	0.16%	0.00%	54.19%
Total (Pixels)	48636	36413	44956	350	7535

Source: The authors.

**Chart 11: Agreement matrix (in percentages) for Landsat-5 classified images from 2011-08-13.**

Classified without NDVI	Classified with NDVI				
	Urban Space	Vegetation	Pasture	Water	Open Area
Urban Space	92.72%	1.58%	25.40%	1.10%	25.37%
Vegetation	0.27%	97.07%	8.68%	0.00%	2.43%
Pasture	6.03%	0.31%	65.83%	0.00%	20.72%
Water	0.35%	1.04%	0.00%	98.90%	0.00%
Open Area	0.63%	0.00%	0.09%	0.00%	51.48%
Total (Pixels)	37750	43215	51967	272	4686

Source: The authors.

Quantitative data suggest that Landsat land use maps caused errors identified by comparison in Chart 12, in which all four 2016 classifications were compared. Such errors may be attributed to the omission of data related to the images' spatial resolution, as the digital number in each pixel derives from the mean of all information contained in a given location. Considering the bands chosen in Landsat imagery, each pixel represents a 900 m<sup>2</sup> area. As all the information in every pixel's corresponding area is condensed into a digital number, all categories in Landsat image classification show significantly greater error levels than those in Sentinel imagery, where each pixel accounts for only 100 m<sup>2</sup>. Nonetheless, the quantitative information produced provides a database for Ipiranga Creek. Changes in the five image classification categories in the chosen time period reflect development in the basin over the past 18 years.

**Chart 12: Quantitative summary for classes with and without NDVI.**

Without NDVI				
Categories of classification	Area of each category (in km <sup>2</sup> )			
	1999-08-12 LANDSAT-5	2011-08-13 LANDSAT-5	2016-07-25 LANDSAT-8	2016-07-13 SENTINEL-2A
Urban Space	8.37	7.35	9.32	6.65
Vegetation	4.44	5.26	4.61	4.77
Pasture	7.10	7.86	6.90	9.79
Water	0.02	0.01	0.01	0.01
Open Area	1.41	0.85	0.49	0.14
With NDVI				
Categories of classification	Area of each category (in km <sup>2</sup> )			
	1999-08-12 LANDSAT-5	2011-08-13 LANDSAT-5	2016-07-25 LANDSAT-8	2016-07-13 SENTINEL-2A
Urban Space	8.67	9.32	10.44	6.31
Vegetation	5.02	5.87	5.11	5.83
Pasture	6.42	5.66	5.39	9.04
Water	0.12	0.03	0.01	0.01
Open Area	1.10	0.46	0.39	0.16

Source: The authors.

## 5 CONCLUSIONS

Landsat series NDVI-enabled classification produced small errors caused by shadows in the scenery, which were confused with water and open areas. However, no such confusion was registered in classified Sentinel-2 imagery, in which case NDVI-enabled classification yielded more reliable results.

The data in this paper may be used to assess historical changes in the drainage basin. In the last 18 years, urban space and vegetation have not shown any considerable deviation from the magnitude of approximately 6 km<sup>2</sup>. Pasture grew to 9 km<sup>2</sup>, water has not shown any increase and open areas shrunk considerably.

All data collected by following the presented methodology may be used as historical reference for the region's environmental planning and control, as it has been shown that these values are fully coherent with actual data obtained within the region's perimeter.

Pasture areas were directly affected by several land development projects over the last few years, leading to an increase in surface runoff and more aggressive floods in the basin's plains. This is the greatest challenge to society and government officials, as it worsens the quality of life of the population.

Use of MapBiomias, a QGIS software plugin, is a good way to continue monitoring the area. The results in this paper may be compared to future ones as a means of improving the analysis of the region, since the aforementioned plugin's database goes back as far as 1985.

## 6 ACKNOWLEDGMENTS

We would like to thank the Center for Geoenvironmental Analysis (NAGEA) and the Federal University of Juiz de Fora (UFJF).

## 7 BIBLIOGRAPHICAL REFERENCES

ALVES, G. B. M.; LOVERDE-OLIVEIRA, S. M. Uso do índice de vegetação por diferença normalizada (NDVI) para análise da distribuição e vigor da vegetação no pantanal norte. *GEOGRAFIA (Londrina)*, v. 29, p. 1-175, 2020.

BARRA ROCHA, C. H.; FREITAS, F. A. DE; CASQUIN, A. P. Conflitos de uso da terra nas APPs hídricas de manancial da zona da mata mineira, BRASIL. *Boletim Goiano de Geografia*, v. 39, n. 0 SE-Artigos, p. 1–22, 2019. Available at: <<https://revistas.ufg.br/bgg/article/view/50021>>.

BEZERRA, U. A.; OLIVEIRA, L. M. M.; CANDEIAS, A. L. B.; SILVA, B. B.; LEITE, A. C. S.; SILVA, L. T. M. S. Comparativo do Índice de Vegetação de Diferença Normalizada (NDVI) entre os sensores OLI - satélite Landsat-8 e MSI satélite Sentinel-2 em região semiárida. *Anuário do Instituto de Geociências - UFRJ*, v. 41, p. 167-177, 2018.

CABRAL, E. G.; BARREIRA, S.; FERREIRA, M. E.; ARAÚJO, L. G. DE O. A silvicultura do eucalipto no estado de Goiás: um registro histórico via sensoriamento remoto. *Pesquisa Florestal Brasileira*; v. 39 (2019), 2019. Available at: <<https://pfb.cnpf.embrapa.br/pfb/index.php/pfb/article/view/1649/907>>.

DURAN, D. C.; GOGAN, L. M.; ARTENE, A.; DURAN, V. The Components of Sustainable Development - A Possible Approach. *Procedia Economics and Finance*, v. 26, p. 806–811, 2015. Available at: <<http://www.sciencedirect.com/science/article/pii/S2212567115008497>>.

DURAN, M.; HERNÁNDEZ, M.; REBECA, G.; ÁLVAREZ-ARTEAGA, G. Cambio de uso de suelo e índice de vegetación de diferencia normalizada (NDVI), subcuena del río salado, MÉXICO. *Geografía y Sistemas de Informacion Geografica*, v. 9, p. 39–50, 2017.

INPE – Instituto Nacional de Pesquisas Espaciais. (2021). Website: <<http://www.dgi.inpe.br/CDSR/>>. Viewed 15 March 2021.

LANDIS, J. R.; KOCH, G. G. The Measurement of Observer Agreement for Categorical Data. *Biometrics*, v. 33, n. 1, p. 159–174, 1977. [Wiley, International Biometric Society]. Available at: <<http://www.jstor.org/stable/2529310>>.

LEANDRO, D.; SANTOS, D. B.; DALLMANN, D. K., Uso e ocupação do solo no município de Cristal/RS. *Revista Iberoamericana de Ciências Ambientais*, v. 10, p. 340-350, 2019.

MOREIRA, E. P.; RODRIGUES, T. G.; OLIVEIRA, C. G.; SILVA JUNIOR, J. A.; OLIVEIRA, V. M. Análise de dados OLI/Landsat-8 e MSI/Sentinel-2 com diferentes níveis de processamento. *Brazilian Journal of Development*, v. 6, p. 35820-35831, 2020.

NETO, R. M.; OLIVEIRA, G. C.; RODRIGUES, E. L. N.; OLIVEIRA, A. Geossistemas: interpretação e aplicação de um conceito para uma proposta de zoneamento ambiental na bacia do rio paraibuna, Zona da Mata mineira. *Caminhos da Geografia (UFU. Online)*, v. 18, p. 90-109, 2017.

NGUYEN, T. T.; VERDOODT, A.; VAN Y, T.; et al. Design of a GIS and multi-criteria based land evaluation procedure for sustainable land-use planning at the regional level. *Agriculture, Ecosystems & Environment*, v. 200, p. 1–11, 2015.

DE OLIVEIRA, D. E.; DE ASSIS, D. C.; FERREIRA, C. DE C. M. Dinâmica climática regional em municípios da zona da mata, campo das vertentes e sul e sudoeste de Minas Gerais: As ondas de calor e frio. *Revista Brasileira de Climatologia; DOSSIÊ CLIMATOLOGIA DE MINAS GERAISDO* - 10.5380/abclima.v1i0.61039, 2018.

RELATÓRIO ANUAL DE DESMATAMENTO 2019 – São Paulo, SP – MapBiomass, 2020. 49 p.

ROBINSON, N. P.; ALLRED, B. W.; JONES, M. O.; et al. A Dynamic Landsat Derived Normalized Difference Vegetation Index (NDVI) Product for the Conterminous United States. *Remote Sensing*, 2017.

Rouse, J.W; Haas, R.H; Schell, J. A; Deering, D. W. Monitoring vegetation systems in the Great Plains with ERTS. In: *Proceedings of the 3rd. ERTS-1 Symposium*; 1973; Washington, DC. Washington, DC: NASA SP-351; 1973. p.309-17.

Ruiz Durán, M. E.; Orozco Hernández, M. E.; Granados Ramírez, R.; Álvarez Arteaga, G. 2017. Cambio de uso de suelo e Índice de Vegetación de Diferencia Normalizada (NDVI), subcuenca del río Salado, México. *Geografía y Sistemas de Información Geográfica (GeoSIG)*. 9(9), section I:39-50.

SILVEIRA, A. H. DE M.; SILVA, F. M. DA; HADAD, R. M.; LIBÓRIO, M. P. Aplicações, preferências e comparações entre métodos de classificação supervisionada: O caso de NATAL/RN. *Raega - O Espaço Geográfico em Análise*; v. 47, n. 1 (2020) DO - 10.5380/raega.v47i1.67845 , 2020. Avaliable at: <<https://revistas.ufpr.br/raega/article/view/67845>>.

SOTHE, C.; ALMEIDA, C. M.; LIESENBERG, V.; SCHIMALSKI, M. B. Evaluating Sentinel-2 and Landsat-8 Data to Map Sucessional Forest Stages in a Subtropical Forest in Southern Brazil. *Remote Sensing*, 2017.

WCED. *Our common future*. Oxford; New York: Oxford University Press, 1987.

WECKMÜLLER, R; ZEBENDE, J. V. J; VICENS, R. S. Escolha do melhor descritor para a detecção de trajetórias em florestas tropicais utilizando os algoritmos Landtrendr. *Revista Continentes*, [S.l.], n. 13, p. 68-84, Feb. 2019.

UNITED STATES GEOLOGICAL SURVEY (USGS). Using the USGS Landsat 8 Product. Avaliable at: <<https://www.usgs.gov/core-science-systems/nli/landsat>>. Viewed 16 March 2021.